npj | science of learning

Article

Published in partnership with The University of Queensland

https://doi.org/10.1038/s41539-025-00316-3

Understanding the role of eye movement pattern and consistency during face recognition through EEG decoding

Guoyang Liu[1,2], Yueyuan Zheng[2,3], Michelle Hei Lam Tsang[2], Yazhou, Zhao[2] & Janet H. Hsiao[2,3,4]

Eye movement patterns and consistency during face recognition are both associated with recognition performance. We examined whether they reflect different mechanisms through EEG decoding. Eighty-four participants performed an old-new face recognition task with eye movement pattern and consistency quantified using eye movement analysis with hidden Markov models (EMHMM). Temporal dynamics of neural representation quality for face recognition were assessed through decoding old vs new faces using a support vector machine classifier. Results showed that a more eye-focused pattern was associated with higher decoding accuracy in the high-alpha band, reflecting better neural representation quality. In contrast, higher eye movement consistency was associated with shorter latency of peak decoding accuracy in the high-alpha band, which suggested more efficient neural representation development, in addition to higher ERP decoding accuracy. Thus, eye movement patterns are associated with neural representation effectiveness, whereas eye movement consistency reflects neural representation development efficiency, unraveling different aspects of cognitive processes.

The ability to efficiently and accurately recognize or identify a face is of vital importance in daily social interactions. Previous studies have reported that averaging across individual participants' eye movements to faces produces a classic T-shaped distribution covering facial features, with fixations more densely covering the eyes than the nose and mouth[1]. Extensive research has delved into the role of eye movements in face recognition, shedding light on the importance of different facial features in face recognition[2–4]. In particular, it has been reported that the optimal recognition performance could be attained with two fixations, with a preferred location just below the eyes[5]. Forced fixations away from this location during face recognition have been shown to decrease recognition performance[6]. In line with these findings, multiple studies have suggested that enhanced identification performance of faces is closely associated with increased attention to the eye region[7,8]. While these findings have enhanced our understanding of general information processing strategies for face recognition in the population, the understanding of how individual differences in attention strategies, as reflected in eye movement behavior, contribute to differences in face recognition performance is still limited[9].

Indeed, eye movements in face recognition have been shown to be highly idiosyncratic. For instance, individuals have preferred fixation locations across different face viewing tasks[10–12]. Moreover, these patterns persist over time, suggesting a consistent strategy or preference that individuals employ when viewing faces[6,13]. These individual differences in eye movement strategies have been shown to be directly associated with recognition performance. For example, a machine learning method-based approach, eye movement analysis with Hidden Markov Models (EMHMM), has been proposed to quantify individual differences in eye movement pattern[10,14,15]. Applying EMHMM to eye movements in face recognition has revealed two primary eye movement patterns: eyes-focused and nose-focused patterns[16–18]. Intriguingly, individuals who adopt the eyes-focused pattern are shown to perform better in face recognition tasks[19,20], which is consistent with prior research suggesting that the eyes are the most diagnostic feature for face recognition[5,7,8].

Most recently, in addition to eye movement patterns, the consistency of eye movements has been shown to play an important role in face recognition performance. Eye movement consistency refers to the degree of regularity or predictability in a person's eye movement across face recognition trials. Using EMHMM, it can be quantified using the entropy of a Hidden Markov Model (HMM) that summarizes a person's eye movement in a visual task. A lower entropy value indicates a higher level of consistency. Recent research has found that higher eye movement consistency (i.e., lower entropy), but not more eye-focused eye movement patterns, is associated with better face

[1]School of Integrated Circuits, Shandong University, Jinan, China. [2]Department of Psychology, University of Hong Kong, Hong Kong, China. [3]Division of Social Science, Hong Kong University of Science & Technology, Hong Kong, China. [4]Department of Computer Science and Engineering, Hong Kong University of Science and Technology, Hong Kong, China. e-mail: jhhsiao@ust.hk

recognition performance in children[21]. This phenomenon is in contrast to the finding from adults, where both eye movement pattern and consistency were associated with recognition performance, with eye movement pattern being a stronger predictor[21,22]. While these findings suggest that both eye movement patterns and consistency contribute to an individual's face recognition performance, it remains unclear whether they reflect different mechanisms underlying face recognition. More specifically, since eye movement patterns are directly relevant to the quality of the facial features extracted for face recognition whereas eye movement consistency reflects whether an efficient visual routine has been learned, we speculated that eye movement patterns may be particularly associated with individual differences in the quality of the neural representation for effective face recognition, whereas eye movement consistency may be particularly relevant to the efficiency of the formation of such neural representation.

To test this hypothesis, here we examined participants' neural representations for face recognition as measured in Electroencephalography (EEG). EEG is a well-established and non-invasive neuroimaging tool widely used in neuroscience and is particularly suitable for examinations on the temporal dynamics of neural representations in a cognitive task due to its excellent temporal resolution[23,24]. Most previous studies examining neural correlates of face recognition using EEG focused on univariate analyses of event-related potential (ERP) components, including N170, N250, N400, and P600[25]. In general, the N170 component was found to be associated with face structural encoding[26], followed by the N250 component reflecting activation of the visual face memory[27]. The later ERP components, N400 and P600, were shown to play an important role in more advanced processing stages, with N400 related to personal semantic information processing and P600 associated with reevaluation or integration of facial information[28]. Note that ERP component analysis typically focuses on a small number of electrodes in a specific localized region. However, activations across different regions of the brain have been found to contribute jointly to face recognition processes[29–31]. Therefore, multivariate pattern analysis (MVPA) has been adopted in a few studies to decode neural representations of faces by utilizing multiple electrodes[32,33]. It enables analysis and visualization of the overall dynamics of brain activities by decoding EEGs important for face recognition at each time point across electrodes, providing a detailed time course and topography of neural representation changes during face recognition. In addition, ERP analysis primarily reflects phase-locked, lower frequency activities associated with the stimulus, and thus could miss non-phase-locked brain activities in higher frequency bands. In contrast, EEG spectral analysis could reveal neural activities across different EEG bands.

Previous research has suggested that information in the EEG alpha band (8–12 Hz) is particularly relevant to face perception and recognition processes. For example, it was found to be associated with attentional control processes when anticipating faces vs other objects[34], where attention to faces selectively decreased alpha band power. EEG alpha band information is also found to be associated with the perception of emotional facial expressions, with higher alpha-band responses associated with more neutral emotions[35,36]. Evidence from event-related desynchronization and synchronization (ERD/ERS) analysis also indicated that alpha band signals were related to episodic recognition memory for faces[37]. Some studies have further separated the alpha band into higher (8–10 Hz) and lower alpha (10–12 Hz) bands since they were shown to reflect different cognitive processes. More specifically, lower alpha band information is more relevant to attentional task demands, whereas upper alpha band reflects memory performance and intelligence[38,39]. Some studies have used machine learning-based classification approaches to decode neural representations for familiar vs unfamiliar face recognition and found that EEG alpha band contained discriminative features for face recognition[40–43]. Together, these findings suggest that in addition to the ERP components mentioned above, EEG alpha band information may be particularly relevant to neural representations for face processing. In addition, decoding neural representations through machine learning methods may help us better understand individual differences in neural representations for face processing. Thus, these measures and approaches are particularly suitable for the current examinations on the relationship between eye movement behavior and neural representations for face recognition.

Indeed, some previous EEG studies have reported associations between eye movements and neural representations related to face processing. For example, in ERP studies, N170 amplitude is significantly enhanced when participants focusing on the eyes as compare with focusing on the nose or mouth[44,45] or viewing the configuration of the whole face[46–48]. Moreover, it was shown that N170 and P300 information could be used to uniquely distinguish eye contact from other responsive facial movements, and these responses were correlated with individual variability in social function[49]. EEG/ERP measures have also been shown to be associated with face recognition performance. For example, N170 latency has been demonstrated to correlate with recognition accuracy[50]. Using EEG decoding methods, it has been reported that errors in decoding face identities and facial expressions were significantly correlated with errors in behavioral performance[51]. Similarly, accuracy in decoding face familiarity was correlated with mean reaction time in a face matching task[52]. Together, these findings suggested that EEG signals recorded during face recognition are sensitive to both face recognition performance and related eye movement behavior, and thus are ideal for the examination on the association between individual differences in neural representations and eye movement behavior during face recognition.

In this study, we aimed to examine the neural information processing mechanisms underlying the association between eye movement pattern/consistency and face recognition performance. More specifically, we examined the associations between individual differences in eye movement pattern and consistency during face recognition and temporal dynamics of the neural representation for face processing as indexed by the performance of machine learning methods in decoding face recognition using both ERP and EEG data. Through EEG decoding, we first examined what EEG signals contain significant features and information for successful face recognition. We then used both decoding accuracy and its peak latency to assess the decoding performance[32] and examine how they were associated with individual differences in eye movement pattern and consistency, while controlling for variance due to possible associated cognitive ability factors. In particular, the alpha band of EEG signals is of interest due to its relevance to attentional effects in visual tasks, including face recognition tasks[53,54]. Accordingly, we hypothesize that ERP and alpha band signals may contain informative features for EEG decoding of old/new face recognition, and a more eyes-focused eye movement pattern and more consistent eye movement behavior (lower entropy) would be associated with better effectiveness of neural representation measured by decoding accuracy and efficiency of neural representation development reflected in the decoding latency.

Results

Eye movement patterns in face recognition

Using the EMHMM analysis, we discovered two representative eye movement patterns as the result of clustering: the eyes-focused and nose-focused patterns (Fig. 1). This finding was consistent with previous EMHMM studies on face recognition[14,16,17,19,20,55]. After the first fixation at the face center/red region of interest (ROI) (83% probability) due to the drift check prior to the face presentation, participants adopting the eyes-focused pattern typically started to fixate on the eye region including left eye/green ROI (56%) and right eye/blue ROI (31%). Afterwards, they most likely switched to the other eye (left eye to right eye, 55%; right eye to left eye, 43%), and occasionally switched to the mouth region/pink ROI (left eye to mouth, 22%; right eye to mouth, 32%). In contrast, participants adopting the nose-focused pattern started at the center of the face (red ROI: 52%; cyan ROI: 47%) and mainly looked around the face center with broad ROIs. The two representative HMMs differed significantly[14]: data from those with the eyes-focused pattern were more likely to be generated from the eyes-focused than nose-focused representative HMM, $t(30) = 14.35$, $p < 0.001$, $d = 2.58$, and data from those using the nose-focused pattern were more likely to be generated from the nose- focused than the eyes-focused representative

Fig. 1 | The EMHMM clustering results. The eye-focused and nose-focused patterns are generated. **a** The eye-focused patterns generated by EMHMM. **b** The nose-focused patterns generated by EMHMM. Ellipses show ROIs as 2-D Gaussian emissions. The table shows transition probabilities among the ROIs. Priors show the probabilities that a fixation sequence starts from the ellipse. The image in the middle shows the corresponding heatmap.

a Eyes-focused pattern (31 models)

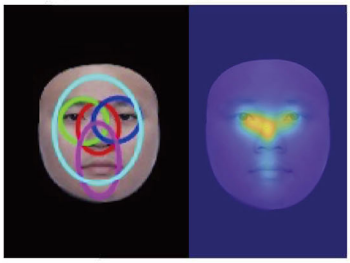

Eyes-focused	To Red	To Green	To Blue	To Pink	To Cyan
Priors	.83	.00	.00	.00	.17
From Red	.00	.56	.31	.06	.07
From Green	.00	.03	.55	.22	.20
From Blue	.00	.43	.04	.32	.20
From Pink	.00	.23	.00	.03	.74
From Cyan	.00	.00	.00	.00	1.0

b Nose-focused pattern (53 models)

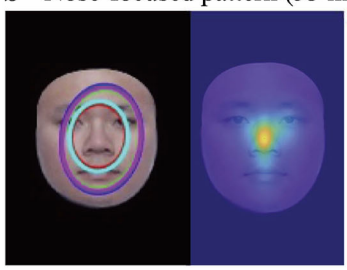

Nose-focused	To Red	To Green	To Blue	To Pink	To Cyan
Priors	.52	.00	.01	.00	.47
From Red	.00	.52	.18	.30	.00
From Green	.00	.07	.64	.29	.00
From Blue	.00	.05	.78	.17	.00
From Pink	.00	.04	.87	.09	.00
From Cyan	.00	.53	.17	.30	.00

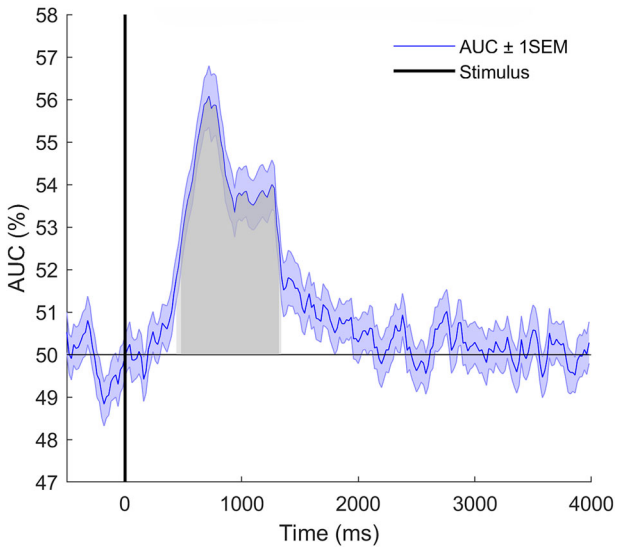

Fig. 2 | AUC performance curve for ERP decoding (0.5–6 Hz). The black horizontal line represents the chance level performance (AUC = 0.5), and the black bold vertical line indicates the stimulus presentation onset time. The AUC values in the shaded area are significantly higher than the chance level, where the light gray area indicates the area with corrected $p < 0.05$, and the dark gray area indicates the area with corrected $p < 0.001$. The purple shading indicates ±1 standard error of the mean (SEM).

HMM, $t(52) = 3.12$, $p = 0.002$, $d = 0.43$. To be consistent with previous studies, here we refer to A–B scale as the eyes-nose scale. For a more specific definition of the A–B scale, please refer to "Eye-movement analysis".

Group-level EEG decoding performance analysis results

We conducted ERP decoding and alpha band decoding using the support vector machine (SVM) for the 84 participants, and the averaged area under the receiver operating characteristic curve (AUC) performance was measured. Figure 2 shows the AUC performance of the ERP decoding. It can be seen that the average decoding AUC over all participants was significantly higher than the chance level from 440 ms and quickly reached the peak AUC of 0.56 at 720 ms. Then the decoding performance was sharply dropped from 720 ms to 940 ms. After maintaining a relatively low but still highly significantly above chance level decoding performance for 320 ms, the AUC sharply dropped again to the chance level. The significant overlap between dark and light gray areas and the sharp increase and decrease in edges reflected the phase-locked property of ERP responses. The ERP decoding results suggested that the later ERP components, such as N400 and P600 components may play an important role in distinguishing old and new faces, consistent with some previous ERP studies on old/new face recognition memory tasks[56–58] and familiar/unfamiliar face recognition tasks[25,59]. The low- and high-alpha band decoding results are demonstrated in Fig. 3a, b. Because of the phase-independent feature of instantaneous power magnitude[60,61], the decoding performance curves did not have a sharp increase and decrease as the ERP decoding curve, with a relatively lower peak average AUC and a larger AUC peak latency. For the low-alpha band decoding, the time period with significantly above-chance decoding performance ranged from 880 ms to 1720 ms, with corrected p-values less than 0.05 but greater than 0.001. The peak average decoding AUC of 0.53 was achieved at 1240 ms. For the high-alpha band decoding, the time period with above-chance AUC was found from 720 ms to 2020 ms, as well as from 2060 ms to 2160 ms, with the peak AUC of 0.54 occurring at 1080 ms. The time period between 820 ms and 1700 ms had the corrected p-values smaller than 0.001. These results suggested that the high-alpha band contained more discriminative EEG features than the low-alpha band.

Individual-level correlation analysis results

Based on the group-level EEG decoding performance, we computed the time period of interest AUC (TOI-AUC) and the peak latency of decoding AUC for each participant, and individual-level correlation analyses were conducted. The ERP band part of Table 1 shows the results of the correlation analyses between ERP decoding performance measures and other measures, including eye movement, cognitive ability, and face recognition performance measures. It can be seen that the TOI-AUC was negatively correlated with face recognition response time (RT) and eye movement overall entropy (i.e., positively correlated with eye movement consistency). These results suggested that higher ERP decoding accuracy was associated with faster face recognition responses and more consistent eye movements during face recognition.

In the high-alpha band part of Table 1, decoding performance measure TOI-AUC in the high-alpha band was negatively correlated with the eye movement pattern measure A–B scale, indicating that a more eye-focused pattern was associated with a higher EEG decoding accuracy. To better visualize this effect, we contrasted the curves of the decoding performance in

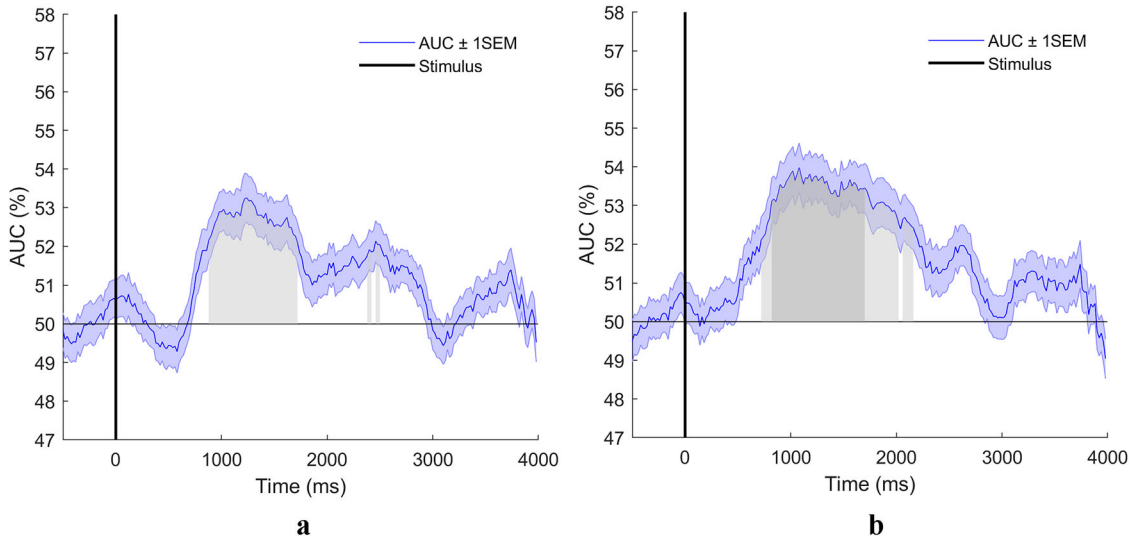

Fig. 3 | AUC performance curve for alpha band decoding (8–12 Hz). The black horizontal line represents the chance level performance (AUC = 0.5), and the black bold vertical line indicates the stimulus presentation onset time. **a** AUC performance curve for low-alpha band decoding (8–10 Hz). **b** AUC performance curve for high-alpha band decoding (10–12 Hz). The AUC values in the shaded area are significantly higher than the chance level, where the light gray area indicates the area with corrected $p < 0.05$, and the dark gray area indicates the area with corrected $p < 0.001$. The purple shading indicates ±1 SEM.

Table 1 | Individual-level correlation analysis

Measure names		ERP decoding measures		Alpha decoding measures		Behavioral performance	
		TOI-AUC	Latency	TOI-AUC	Latency	FR ACC	FR RT
ERP decoding measures	TOI-AUC	1					
	Latency	0.236$^{+,\#}$	1				
Alpha decoding measures	TOI-AUC	0.085	0.046$^{\#}$	1			
	Latency	−0.102	0.013$^{\#}$	0.297**	1		
Behavioral performance	FR ACC	0.005	0.123$^{\#}$	0	0.145	1	
	FR RT	−0.52***	0.098$^{\#}$	−0.045	0.256*	0.055	1
Eye movement measures	AB-Scale	0.11	−0.003$^{\#}$	0.242*	−0.18	0.059	−0.151
	Overall entropy	−0.274*	0.124$^{\#}$	−0.046	0.273*	0.022	0.59***
Cognitive measures	Nonverbal IQ	0.158$^{\#}$	−0.07$^{\#}$	−0.089$^{\#}$	−0.294$^{**,\#}$	0.169$^{\#}$	−0.058$^{\#}$
	WM ACC (spatial)	0.116	−0.045$^{\#}$	−0.022	−0.168	0.145	−0.226*
	WM RT (spatial)	−0.04	0.034$^{\#}$	0.097	0.025	0.19^{+}	0.075
	WM ACC (verbal)	−0.201$^{+,\#}$	−0.133$^{\#}$	0.078$^{\#}$	−0.007$^{\#}$	0.036$^{\#}$	0.12$^{\#}$
	WM RT (verbal)	−0.109	0.055$^{\#}$	−0.123	−0.048	0.146	0.122
	ToL planning	−0.105	0.134$^{\#}$	−0.078	0.08	0.293**	0.246*
	ToL executing	−0.141	−0.032$^{\#}$	0.101	0.106	0.062	0.01
	ToL total time	−0.191^{+}	0.02$^{\#}$	0.042	0.144	0.235^{+}	0.16
	ToL total move	−0.001	−0.113$^{\#}$	0.082	0.137	−0.2^{+}	−0.104

Alpha decoding measures show the measures from the high-alpha band.
FR ACC face recognition accuracy, *FR RT* face recognition response time, *WM ACC* working memory accuracy, *WM RT* working memory response time, *ToL* tower of London.
$^{+}$Marginally significant correlation with $0.05 < p < 0.1$.
*Significant correlation with $0.01 < p < 0.05$.
**Significant correlation with $0.001 < p < 0.01$.
***Significant correlation with $p < 0.001$.
$^{\#}$Spearman correlation.

AUC of the participants in the two eye movement groups in Fig. 4, where all *p*-values are corrected using the BH method. It can be seen that, consistent with the observed correlation, the decoding performance of the eyes-focused group was higher than that of the nose group for most of the time points during 800 ms to 2100 ms after the stimulus onset. Regarding decoding peak latency, we found a positive correlation between decoding peak latency and face recognition RT. Additionally, it was positively correlated with eye movement entropy and negatively correlated with non-verbal IQ, suggesting that the later the latency, the more inconsistent the eye movement behavior and the lower the IQ. In this experiment, all participants were

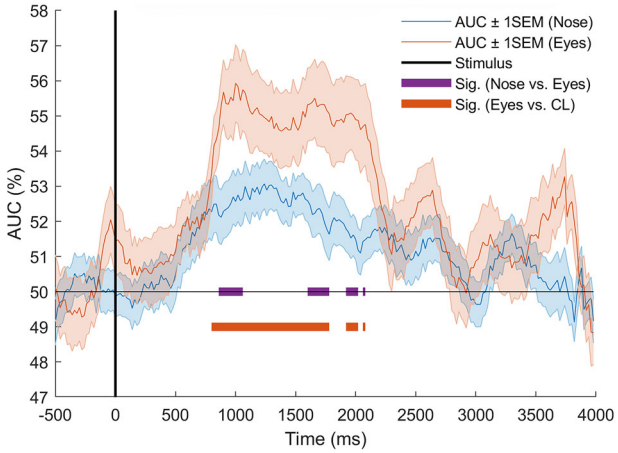

Fig. 4 | Group-wise decoding performance in AUC in the high-alpha band (10–12 Hz) across time points. The black horizon line represents the chance level performance (AUC = 0.5), and the black bold vertical line indicates the stimulus presentation onset time. The bold purple line marks the time period where the eyes-focused group's performance is significantly higher than the nose-focused group's performance (corrected $p < 0.05$). The bold red line marks the period which the eyes-focused group's performance is significantly higher than the chance level (corrected $p < 0.05$). The blue and orange shading indicates ±1 SEM, and CL indicates the chance level.

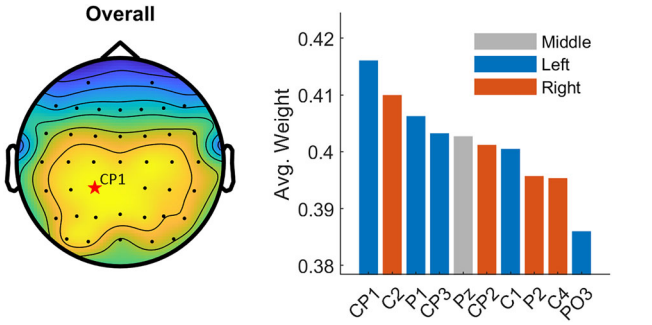

Fig. 5 | Averaged topography map in the ERP band. The left subplot shows the topography map, while the right subplot illustrates the top-10 average weights and their corresponding channels.

found to have a normal intelligence level according to the 9-item Raven's Progressive Matrices (Bilker et al.[62]; $M = 8.00$, $SD = 1.23$). Consistent with our finding, previous research has reported that EEG features from the alpha band were associated with non-verbal intelligence[63]. Together, these findings in the high alpha band suggested that eye movement patterns during face recognition, as measured in A–B scale, were associated with the effectiveness of the neural representations for distinguishing old vs new faces in face recognition memory as reflected in EEG decoding AUC. In contrast, eye movement consistency as measured in entropy was associated with the efficiency of the neural representations as reflected in EEG decoding peak latency (see detailed discussions in "Discussion").

To further examine whether eye movement behavior significantly contributed to decoding performance after variance due to cognitive abilities was controlled, a two-stage hierarchical multiple regression was conducted to predict the peak latency measure of high-alpha band decoding. In addition to eye movement consistency, non-verbal IQ was also significantly correlated with decoding peak latency in the high-alpha band, $r(84) = 0.294$, $p = 0.007$. At the first stage, we added the non-verbal IQ measure into the regression model, achieving a significant contribution and accounting for 9.3% of the variance, $B = 0.305$, $F(1, 82) = 8.38$, $p = 0.005$. At the second stage, introducing eye movement consistency explained an additional 5.4% of the variance in decoding latency, and this change in R^2 was significant, $B = 0.235$, $F(1, 81) = 5.150$, $p = 0.026$. The tests for multicollinearity suggested a low level of multicollinearity (tolerance = 0.981 for both two tested measures). It indicated that eye movement consistency significantly contributed to the peak latency of high-alpha band decoding accuracy after controlling for variance due to non-verbal IQ.

From Table 1, we can see that in all EEG bands, a positive correlation between decoding latency and accuracy was observed. This phenomenon suggested that a longer decoding time may allow for more detailed processing of facial information, leading to higher accuracy. Another interesting observation was that in the ERP band, decoding accuracy was negatively correlated with face recognition reaction time but positively correlated with decoding peak latency in the ERP band. While decoding latency reflects neural processing efficiency of face stimuli, face recognition reaction time represents efficiency in making conscious decisions of the recognition. In other words, a longer neural processing time does not necessarily lead to longer face recognition reaction time.

Feature importance analysis results

By analyzing the weights in the trained SVMs for EEG decoding (see details in "Feature importance analysis"), the topography map for ERP decoding is computed and shown in Fig. 5. The results showed that the electrodes in the central and parietal areas contributed the most to the neural representations for face recognition. This result was consistent with findings in previous studies showing that late ERP responses such as N400 and P600 for face processing were widely distributed in the central and parietal areas[58,59]. Also, previous neuroimaging studies reported that the parietal region participated significantly in face processing[64,65]. Similarly, the average topography map for high-alpha band decoding, illustrated in Fig. 6a, shows that the central and parietal areas were crucial for high-alpha band decoding. Since our results demonstrated an interesting correlation between the decoding performance of high-alpha band information and eye movement patterns, we further plotted and analyzed the topography maps of the two eye movement pattern groups in Fig. 6b, c. As shown in the figure, in participants in the nose-focused group, electrodes in the left central and parietal region contributed more to the neural representation for face recognition, whereas in eyes-focused participants, electrodes in the right central region contributed more. Previous research has suggested that alpha band power in the right-parietal cortex reflects the strength of task-focused attention[66,67]. Besides, neural responses selectively to faces were reported to be mainly in the right occipital-temporal cortex[68] and right occipital cortex[69]. These findings were consistent with our current results that in participants adopting the eyes-focused pattern, which was associated with higher EEG decoding accuracy in the high alpha band, neural representations from the right hemisphere contributed more to face recognition performance.

Discussion

In the current study, we examined the neural information processing mechanisms underlying the association between eye movement pattern/consistency and face recognition performance through ERP and EEG decoding methods. With EMHMM, two dominant eye movement patterns (the eyes-focused and the nose-focused patterns) during face recognition were identified, which were consistent with the previous research. We found that a more eye-focused pattern was associated with more discriminative information for face recognition in the high alpha band signals (as reflected in AUC). In contrast, a more consistent eye movement pattern for face recognition was associated with both higher ERP decoding accuracy and higher EEG decoding efficiency (as reflected in the latency of peak AUC) in the high alpha band for face recognition. These findings support our hypothesis that ERP and EEG alpha band signals contain information important for the decoding of old vs new faces, and eye movement patterns and consistency during face recognition are associated with effectiveness and efficiency of the neural representation for face processing, respectively. In this section, we will delve deeper into these findings, elaborating on the implications of these

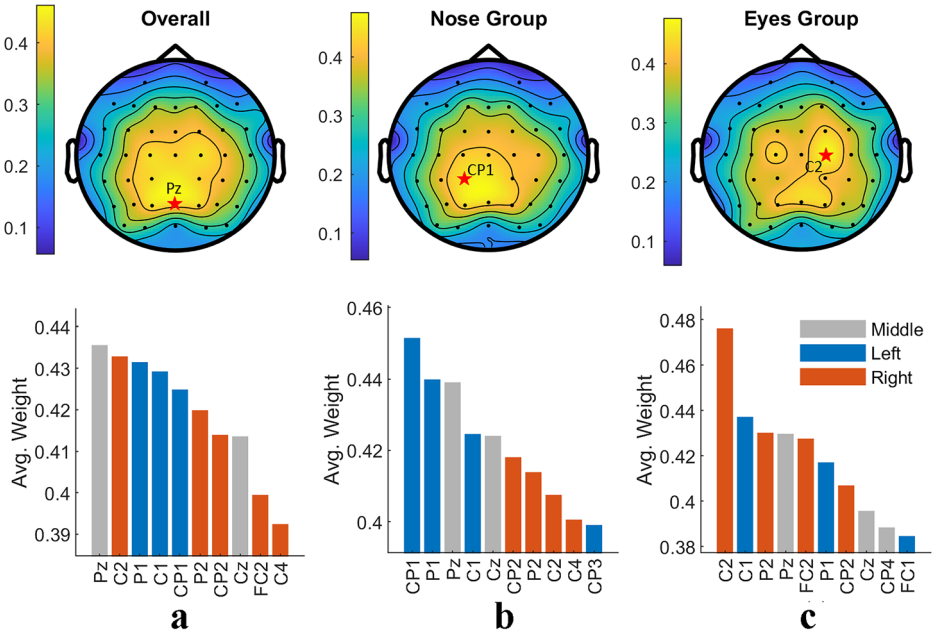

Fig. 6 | Averaged topography maps in the high-alpha band. The topography maps (upper row) and bar charts (lower row) illustrate the distribution of the channel weights. **a** The overall topography map and its top-10 channel weights. **b** The nose group topography map and its top-10 channel weights. **c** The eyes group topography map and its top-10 channel weights.

results based on our hypotheses and existing literature, and further visualizing the specific brain regions contributing the most to decoding accuracy and their associations with eye movement behavior.

Our individual-level analysis results showed that the eyes-focused eye movement pattern was positively correlated with the decoding accuracy measured by TOI-AUC in the high alpha band. Although in the current study, no correlation was observed between eye movement pattern and face recognition accuracy, previous studies have consistently reported that eye-focused eye movement patterns were associated with better face recognition accuracy[7,8,12]. These findings thus suggested that eye movement patterns may be more relevant to the quality of the neural representation for face recognition. In contrast, eye movement consistency was significantly correlated with both the decoding accuracy measured by TOI-AUC in the ERP band and the decoding efficiency measured by latency of the peak AUC in the high alpha band. This result suggests that eye movement consistency may be relevant to both the quality and the efficiency of neural representation for face recognition. In addition, we found a strong positive correlation between eye movement consistency and reaction time of face recognition ($r(84) = 0.59$, $p < 0.001$), indicating that a more consistent eye movement pattern was associated with reduced face recognition time. Together, these findings suggest that eye movement consistency may be particularly relevant to the efficiency of face recognition processes. Consistent with our findings, prior research has shown that in adult face recognition, although both eye movement consistency and eye-focused eye movement pattern were associated with face recognition accuracy, eye movement pattern was a better predictor for recognition accuracy because it accounted for additional variance beyond eye movement consistency[21]. Our current EEG decoding study further showed that eye movement consistency reflected the neural processing efficiency of face processing better than the eye movement pattern. This finding is consistent with previous research suggesting that high eye movement consistency is resulted from a well-learned face scanning routine through experience[21].

The EEG alpha band signals have been implicated in attentional processes, specifically in the inhibition of distracting information[70,71]. In addition, alpha oscillations are thought to reflect the synchronization of neuronal activities in the cortex and have been shown to be modulated by attention[72]. Therefore, a possible explanation for the association between eye movement patterns and alpha-band EEG decoding accuracy is that eye movements help direct attention to the most relevant features for face recognition, which in turn enhances the quality of the neuronal representations for old and new faces, leading to enhanced decoding accuracy. On the other hand, the relationship between eye movement consistency and decoding efficiency may reflect attentional processes in extracting relevant information to face recognition from eye fixations. If attention is constantly diverted to different parts of a face across trials due to a poorly learned visual routine (i.e., low eye movement consistency), this may lead to less efficient extraction of relevant information, and hence lower decoding efficiency. In contrast, a consistent visual routine may enhancethe efficiency of feature extraction, leading to higher decoding efficiency.

In the current study, ERP/EEG features discriminative for decoding old vs new faces in the face recognition tasks were present at a relatively late time window (500–1200 ms). This finding was generally consistent with previous EEG/ERP studies of face processing. For example, a recent MVPA study for decoding familiar/famous vs unfamiliar faces showed that later ERP responses (400–600 ms) contain discriminative information for familiarity[52]. In another study on EEG-based familiar and unfamiliar face classification, it was found that late ERP components within 1–2 s played a significant role in the neural processing of face recognition[41]. Also, in tasks without a clear task demand, such as passive viewing tasks, differences in ERPs elicited by familiar and unfamiliar faces could be observed in late components, including N400 and P600[25,73]. In contrast to these results, some previous studies using personally familiar faces, such as self faces or faces of family/friends, have observed a significant correlation between some early ERP components, including N170 and N360, and familiar face identification performance[74–76]. Thus, the time window with above-chance decoding accuracy for face processing may depend on the task demand. Future work may examine how task demands modulate decoding accuracy and its relationship with eye movement behavior[77].

Previous studies have suggested potential confounding effects of eye movements on EEG decoding performance, particularly the influence of ocular artifacts such as eyeball dipole rotation and saccadic spike activity[78–80]. In particular, some studies have shown that small fixational eye movements could still affect EEG decoding[81,82]. In view of these, we conducted additional analyses with more rigorous considerations of potential influence from eye movements in Supplementary Notes 1–5 (see Supplementary Information). These additional analyses provided consistent evidence that the observed neural differences between old and new faces were unlikely to be confounded by eye movements. More specifically, neither raw eye movement data nor eye fixation data contained sufficient discriminative information for old/new face recognition. This was supported by decoding analyses using

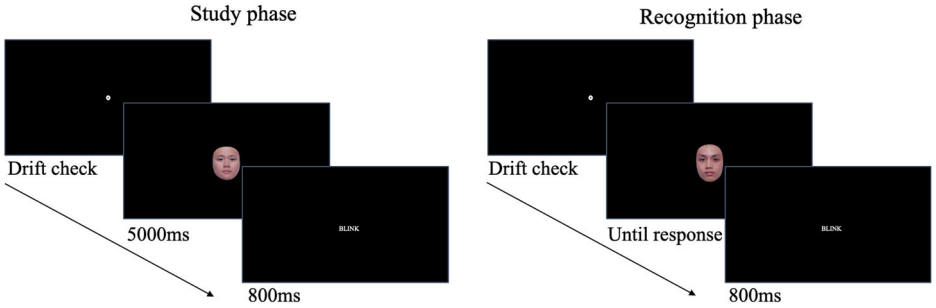

Fig. 7 | The trial procedure of the study and recognition phase of the face recognition paradigm. A trial of the study phase started with a drift check, followed by the face image to be learned that will be presented for 5000 ms, and ended with a screen for blinking. A trial of the recognition phase started with a drift check, followed by a face image to be judged, which would disappear until a response, and ended with a screen for blinking.

the raw eye movement data (Supplementary Notes 1), as well as fixation-based classification with a recurrent neural network model (Supplementary Notes 2), both of which yielded chance-level performance. Additionally, approximations of vEOG and hEOG data failed to decode old vs new faces (Supplementary Notes 3). When they were included as additional channels in our ICA procedure, we obtained similar EEG decoding curves to and consistent findings with our original results (Supplementary Notes 4). Also, we observed no significant difference between old and new face trials in participants' summary statistics measures of eye movements, including average number of fixations per trial and average saccade length (Supplementary Notes 5). Together, these additional analyses confirm that our decoding results genuinely reflected neural responses for face recognition rather than inadvertent oculomotor confounds.

In summary, in this study, we have comprehensively examined the relationship between individual differences in eye movement behavior, including eye movement pattern and consistency, and the temporal dynamics of neural representations in face recognition as indexed by EEG decoding accuracy and its peak latency. We revealed that eye movement behavior is closely associated with the decoding performance of face recognition using information from particularly the EEG high alpha band, confirming the hypothesized relevance of these neural signals in the process of face processing. Specifically, a more eye-focused eye movement pattern was associated with higher decoding accuracy in the high alpha band, suggesting the role of eye movement pattern in shaping the quality of the neural representation for face recognition. In contrast, higher eye movement consistency was associated with a shorter peak latency in high-alpha-band decoding accuracy in addition to higher ERP decoding accuracy, suggesting its role in the efficiency of neural representation development, in addition to the quality. The topographic maps visualizing the trained machine learning classifier (SVM) weights suggested that the central and parietal areas provided the most discriminative features for both the EEG high alpha band decoding and the ERP decoding, with individuals using the eyes-focused pattern showing a more right-brain biased map. These findings demonstrated well the interplay between perceptual strategies and neural representation processing, with eye movement patterns associated with the effectiveness of the neural representations, whereas eye movement consistency reflects the efficiency of neural representation development. Future research will further explore how these insights can be applied in practical settings, such as using eye tracking as a cost-effective method for developing early screening or personalized diagnosis and treatment plans for individuals with face processing or social cognition impairments.

Methods

Participants

We recruited 84 East Asian participants (54 females), aged 18 to 22 years old ($M = 19.95$, $SD = 3.87$) from a local University in Hong Kong. They had normal or corrected-to-normal vision. A power analysis indicated that 84 participants were required for Pearson's correlation analysis, assuming a medium effect size ($f^2 = 0.15$, $\alpha = 0.05$, $\beta = 0.20$). The written informed consent was obtained from all participants. Participants recruited were from independent samples. The methods were performed in accordance with relevant guidelines and regulations, and ethical approval was granted by the Human Research Ethics Committee of the University of Hong Kong for this study (no. EA210427).

Materials and apparatus

Eye movement data were acquired with the SR Research Eyelink Portable Duo. The eye tracker was tripod-mounted and connected to a 510 × 291 cm display monitor with a screen resolution of 1920 × 1080 pixels. A viewing distance of 60 cm was maintained between the monitor and participants' eyes, and their dominant eye was tracked at a sampling frequency of 1000 Hz. Calibration and validation were performed using the default nine-point standard calibration procedure with errors below 1° of visual angle. Drift check was performed before each trial, and recalibration was performed if the offset from the center point exceeded 1° of visual angle. The task was programmed using SR Research Experiment Builder.

Continuous EEGs were recorded using the ANT eego system and ANT waveguard™ caps with 64 Ag/AgCl electrodes placed according to a 10–20 international system configuration. EEGs were acquired at a sampling rate of 500 Hz, with CPz as the online reference and AFz as the ground electrode. Electrode impedance was kept below 20 kΩ, and an electrooculogram was recorded from the left upper cheekbone to monitor eye blinks. Transistor-transistor logic (TTL) signals were sent from the SR Research Experiment Builder program to trigger event markers on the EEG recording in order to synchronize continuous EEGs with the experiment program deployed by the eye tracker.

In the face recognition task, 256 color images of child, young adult, and old adult Asian faces (half male and half female) were used. Frontal face images were cropped according to the face shape, with only inner face features revealed. The original aspect ratio of the images was preserved while the distance between the midpoint of the two eyes and mouth was normalized across all face images. The resulting face stimuli subtended 6° of visual angle horizontally on average, corresponding to the size of a real face with a viewing distance of 2 meters, as recommended by McKone[83].

Experimental design and procedures

Participants completed a face recognition task, three cognitive tasks, and an IQ test. Their eye movements and EEG were recorded in the face recognition task.

For the face recognition task, the experimenter conducted a standard 9-point calibration and validation procedure at the beginning of each block and when the drift check error was larger than 1° of visual angle. Each trial started with a solid circle in the middle of the screen for a drift check, and the experimenter pressed a key to present the stimulus when participants looked at the circle. The face stimulus was presented one at a time at the center of the screen. The face recognition paradigm consisted of two separate phases (see Fig. 7). In the study phase, participants viewed 8 target faces (2 children, 4 young adults, and 2 old adults) in each experimental block, each for 5000 ms, and were instructed to remember them. In the recognition phase, 8 target faces and 8 foil faces were presented in each experimental block. The

face stimulus disappeared when the participant made a key response indicating whether they had previously seen the face or not. A "BLINK" screen was then presented for 800 ms before the end of the trial. Participants rested between blocks. The task consisted of 16 blocks, each of which consisted of 8 target faces and 8 foil faces. The 256 face stimuli were randomly assigned to the 16 blocks accordingly without repetition for each participant, and the stimuli within each block were presented in a random order. Thus, all participants received a different, random order of stimulus presentation. Eye movements and continuous EEGs were recorded during this task. The participants' performance was measured by accuracy, and average reaction time. The accuracy was defined as the portion of the trials with a correct recognition response. The average reaction time was computed using the trials with correct reactions.

Additionally, the detailed descriptions of cognitive tasks and IQ tests are as follows:

Verbal and visuospatial two-back tasks. Two-back tasks[84] were used to assess participants' working memory ability. In the verbal two-back task, numbers were presented at the center of the screen one at a time, and participants judged whether it was the same as the one shown two trials back. In the visuospatial two-back task, different symbols appearing at different locations were presented one at a time, and participants judged whether it appeared at the same location as the one shown two trials back, regardless of the symbol's shape. Each task was conducted in two blocks, and each block included 28 trials. Accuracy and RT were measured for each task.

Tower of London task. Participants' executive function and planning ability were assessed using the Tower of London task[85]. In each trial, participants were presented with figures illustrating a target board and a move board, each with three colored balls randomly distributed across three sticks. The participants were instructed to rearrange the balls on the move board, to match the positions of the balls on the target board. They were told to use the fewest possible moves and to plan before attempting the trial. There were 12 trials in total. An average number of moves, planning time, execution time, and total time were measured.

IQ Raven test. The 9-item Raven's Progressive Matrices[62], adapted from the 60-item Raven's Standard Progressive Matrices[86], was used as an index of participants' nonverbal intelligence. Each test item was a 3×3 matrix of eight black-and-white figures with one missing figure. Participants were required to select the best option out of 6–8 figures to complete the matrix. Participants' total score was computed.

Eye-movement analysis

EMHMM[14] was used to model and quantify the participants' eye-movement patterns in the face recognition task, with both spatial (fixation locations) and temporal (transitions between the locations) dimensions of eye movements taken into account. To ensure the robustness of the model and avoid distortion from extreme values, outlier fixations were identified and excluded. Specifically, any fixation location that deviated more than 2.5 standard deviations from the mean fixation location of a stimulus, either in the vertical or horizontal dimension, was considered an outlier.

We followed previous studies applying EMHMM to face recognition research[18–21,55,87,88] to quantify participants' eye movement patterns. Specifically, each participant's eye movements were summarized with one HMM, which included person-specific ROIs and transition probabilities among these ROIs. A variational Bayesian approach was used to determine the optimal number of ROIs for each individual HMM within a preset range of possible numbers of ROIs from 1 to 6. Each HMM with a specific number of ROIs was trained 300 times, and the HMM with the highest data log-likelihood within the preset range was chosen. A variational hierarchical expectation maximization algorithm[89] was used to cluster the individual HMMs into two groups, Pattern A and Pattern B, based on their similarities, and a representative HMM was generated for each group. The number of ROIs was pre-specified to be the median number of ROIs of the individual HMMs. We clustered the individual HMMs into two groups so that we could calculate the similarities of participants' eye movement patterns to the two contrastive ends, making it easier to quantify the cluster scores. We also tried to determine the optimal number of clusters using a variational Bayesian approach (ref. 15). However, the optimal number of clusters was one, which was less informative as compared with having the two contrastive ends. We conducted paired-sample *t*-tests to check whether the two clusters significantly differed from each other. The clustering procedure was repeated 100 times to select the result with the highest log-likelihood.

Following previous research[14,15], the participants' eye-movement patterns were quantified using the A–B scale, which was defined as $(L_A - L_B)/(|L_A| + |\text{No. } 62401342 \text{ to } G_B|)$, where L_A and L_B represent the log-likelihoods of an individual's eye-movement pattern towards representative Pattern A and Pattern B, respectively. Thus, the A–B scale measures the similarity of an individual's eye movement pattern along the scale, with Pattern A at one end and Pattern B at the other end. A more positive A–B scale indicates a higher similarity to Pattern A, and a more negative A–B scale indicates a higher similarity to Pattern B. In addition, data log-likelihood L_A and L_B were used to evaluate whether the two representative patterns differ significantly from each other: If the two groups indeed differed significantly, data from Pattern A participants should have significantly higher L_A than L_B, and data from Pattern B participants should have significantly higher L_B than L_A[14,15]. Similarly, following previous studies[90–94], eye movement consistency of the participants was assessed by calculating the entropy for each HMM[95]. Higher entropy indicated less predictability, less consistency, and more randomness in the eye movement patterns.

EEG analysis

For the EEG Preprocessing, the EEG data were band-pass filtered from 0.1 Hz to 40 Hz with a 2-order Butterworth IIR filter implemented by the 'pop_eegfiltnew' function in EEGLab, which was a typical setting for EEG analysis[96,97]. After filtering, the ICA was performed to remove blinks and eye movement artifacts. Components associated with blinks and eye movements with a confidence of 99% were identified and discarded by the ICLabel plugin of EEGLab toolbox[98]. For each participant's EEG data, 0–2 ICA components were removed accordingly. Subsequently, the EEG data corrected by ICA were resampled from 500 Hz to 250 Hz to reduce the computational complexity. Then, the resampled continuous EEG data were segmented into trials from −500 ms to 4000 ms, which corresponds to 1125 data points. Note that 500 ms of EEG data before the stimulus was included for each trial as the chance level baseline.

For the EEG decoding, we analyzed the EEG signals with the ERP decoding method for phase-locked information analysis and the EEG instantaneous power decoding methods for phase-independent feature analysis. ERP components mainly exist in the low-frequency band, and thus, the EEG data with frequencies lower than 6 Hz were utilized for ERP decoding[60,61]. For the EEG instantaneous power decoding, an explorative examination was first conducted to determine the frequency bands of interest with a non-overlapping bandwidth of 4 Hz between 4-40 Hz. Statistical analysis results indicated that only the Theta band (4–8 Hz) and the Alpha band (8–12 Hz) had significantly above-chance-level decoding performance for decoding old vs new faces in the face recognition task across continuous time points (see Fig. 8). However, the time period with above-chance-level decoding performance in the Theta band was far less than that in the Alpha band, and the Theta band overlapped with the frequency band used in our ERP decoding analysis. Therefore, we focused on Alpha band analysis for EEG instantaneous power decoding. All EEG bands were extracted using a zero-phase 4-order Butterworth IIR filter implemented by the filtfilt function in MATLAB.

The amplitude of the EEG signals was used as the ERP decoding feature. Specifically, a 5-point moving window was applied non-overlappingly for each trial to compute the averaged amplitude. After performing the averaging procedure, the 1125 time points of each trial were

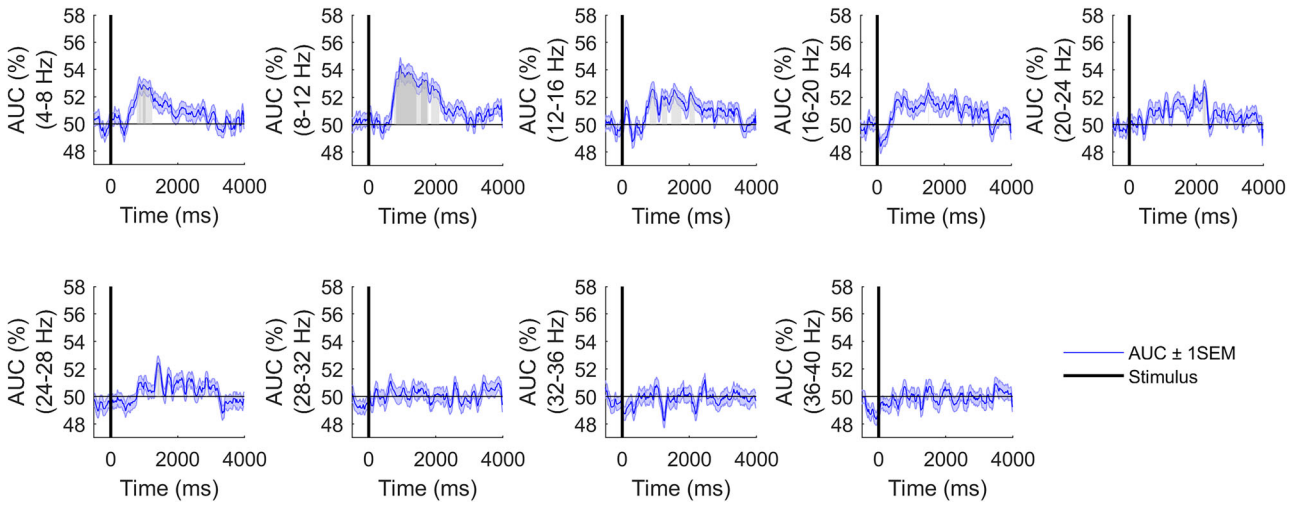

Fig. 8 | The power decoding performance of various frequency bands (4–40 Hz) for decoding old vs new faces. The AUC values in the shaded areas are significantly higher than the chance level: light gray indicates areas with the corrected significance level $p < 0.05$, whereas darker gray indicates areas with the corrected significance level $p < 0.001$. The p-values are corrected by the Benjamini and Yekutieli method.

turned into 225 time points, which further reduced the computational complexity and increased the robustness of instantaneous amplitude estimation. Sequentially, each point of averaged amplitude corresponded to an EEG signal duration of 20 ms. For each participant, we computed the decoding performance at each averaged point.

In order to calculate the instantaneous power for the Alpha band, the Hilbert transform was first applied to each trial of EEG data. Considering the Hilbert transform is suitable for narrowband signal analysis[99,100], we further separated the alpha band into low-alpha band (8–10 Hz) and high-alpha band (10–12 Hz) for analysis to improve the resolution of frequency analysis. For both the low- and high-alpha bands, a complex vector with a length of 1125 time points was obtained for each trial using the Hilbert transform. Then, complex values standing for instantaneous magnitude were squared to compute the instantaneous power of each time point. Each trial of the transformed power data was applied with a 5-point averaging window, in the same way as the window used in ERP decoding, obtaining a processed trial with 225 time points.

To realize decoding old vs new faces in the face recognition task, an SVM with a linear kernel was trained to decode the ERP amplitude features and instantaneous power features of low- and high-alpha bands. The SVM with a linear kernel has low computational complexity, and the weights are interpretable. Besides, the raw classification score output from the SVM was transformed by the logit function $1/(1 + e^{-x})$. In this study, a subject-specific evaluation method was utilized; i.e., the training and testing procedures were conducted separately for each participant using the EEG data. For each participant, we computed the decoding performance from time point to time point to examine the temporal dynamics of decoding performance. To ensure the robustness of the decoding performance, a bootstrapping evaluation strategy was leveraged for the decoding at each time point. Specifically, the feature vector set corresponding to each time point of a trial was randomly divided into a training set (80%) and a validation set (20%). An initial check was conducted before splitting to avoid only one category existing in the training set. There were 63 elements corresponding to 63 channels in one feature vector. Note that trials with wrong responses were eliminated to avoid noisy information. Then, an SVM was trained using the training set, obtaining a binary classifier. Subsequently, this classifier was tested using the validation set to obtain the decoding performance. We repeated the above training and testing procedure 100 times, and the average performance was reported. Given that trials with wrong responses were removed, the training set for each participant was imbalanced. Therefore, AUC was used to measure decoding performance since it is a more robust measure for imbalanced datasets[101]. The AUC score ranges from 0 to 1, where 0.5 indicates the chance level performance. Accordingly, 225 averaged AUC scores were generated for each participant, where the first 25 scores belonged to the pre-stimulus period.

Performance analysis

For the group-level decoding performance analysis, we aimed to examine the temporal characteristics of EEG signals for decoding whether a presented face was a learned/old face or a new face using ERP amplitude and power of the high- and low-alpha bands. Statistical analysis was performed on the data at each time point from the 84 participants to examine whether the decoding achieved above-chance level performance. We used the decoding performance during the pre-stimulus period to define the chance level performance for group-level decoding performance analysis. More specifically, for each participant, the average AUC score over the pre-stimulus period (25 time points) was used as the chance level performance, forming a chance level data group with 84 samples, each corresponding to a participant. For each time point during the post-stimulus period, there were 84 samples of average AUC scores, one from each participant. A two-sided Kolmogorov–Smirnov (K–S) test[102] was used to confirm the normal distribution assumption, and then a pairwise t-test was conducted to examine whether data from each time point during the post-stimulus period were significantly higher than the chance-level data from the pre-stimulus period. Given the multiple statistical tests performed across the time points in this analysis, we used a multiple comparison correction for p-values implemented by a Matlab script[103] using the Benjamini and Yekutieli (BY) method[104]. To comprehensively illustrate the significance test results, two significance level settings at 0.05 (two sided, statistically significant) and 0.001 (two-sided, statistically highly significant), respectively, were reported. In this work, EMHMM was used to analyze the eye movement data of the participants (see the "Eye-movement analysis" for details). To gain deeper insights into the relationship between eye movement behavior and EEG decoding performance, the same group-level significance test and p-value correction procedures were applied to the two participant groups discovered through EMHMM clustering for those EEG bands that showed correlations with eye movement patterns in the EMHMM analysis.

For the individual-level correlation analysis, we aimed to examine the relationship between individual differences in ERP/EEG decoding performance and eye movement behavior for face recognition. We used two ERP/EEG decoding performance measures for each participant, namely the TOI-AUC, where the TOI was defined using the group-level analysis results, and

the peak latency of the decoding AUC within the TOI. More specifically, for the TOI-AUC, the TOI was defined as the time period with average decoding AUC significantly above the chance level ($p < 0.001$) in the group-level analysis described in the "Eye-movement analysis", and the TOI-AUC of each participant was defined as the average AUC within the TOI. TOI-AUC thus reflected the effectiveness of the participant's ERP/EEG responses for decoding old vs new faces. The peak latency of decoding AUC was defined as the time the peak AUC was observed before the participant's average RT, which reflected the decoding efficiency of the participant's ERP/EEG responses. Pairwise correlation analyses were performed between EEG measures and other measures, including both eye movement and cognitive ability measures, and statistically significant correlation coefficients with p-values less than 0.05 were reported. To address the potential for Type I errors due to multiple comparisons in correlation analysis, we applied p-value corrections to the correlations among EEG measure group, eye movement measure group, and behavioral performance group using the Benjamini–Hochberg (BH) false discovery correction procedure[105]. For data that did not meet the normal distribution assumption, the Spearman correlation coefficient was used instead. Hierarchical regression analysis was then used to examine whether eye movement behavior could predict EEG decoding accuracy, with individual differences in cognitive abilities controlled.

We performed a feature importance analysis to visualize the important brain regions in the face recognition task, we examined the importance of each electrode contributing to the classifier used in the EEG decoding processes. The classifier used in the EEG decoding was SVM with a linear kernel, whose trained weights were fully explainable and could directly represent the importance of input features. Previous studies typically used the absolute value of the linear SVM weights to perform feature ranking[106,107]. Accordingly, we examined the linear weights from all the trained SVM models. In each EEG band, a weight matrix w with a size of 63 (channels) × 225 (time points) × 84 (participants) × 100 (testing times on the validation set) was first gathered, and then the element-wise absolute operation was performed on w. Subsequently, an average operation was conducted over the 100 testing times. The weights were normalized to be within 0–1 along the channel dimension for each time point of each participant to control for differences in feature scales across the participants. After that, the time points within the band-specific significance regions (i.e., the time points with decoding accuracy significantly higher than the chance level in the ERP and alpha band) were selected and the mean weight values across the time points were calculated to obtain an individual-level average channel weight for each channel and each participant. The individual-level channel weights were then averaged across participants to obtain a 63-element vector of group-level channel weights, with each element corresponding to a channel. This vector of 63 elements, each representing the average importance of a corresponding channel, was visualized in a topography map according to their locations. We also computed the topography maps for the two eye movement pattern groups separately with the same approach. Note that for this analysis, we only selected the time points with highly significant above-chance decoding performance (with corrected $p < 0.001$), and therefore only the topography of the ERP band and the high-alpha band were computed.

Data availability

The human data for EEG decoding and eye movement analysis of this study are publicly available on the Open Science Framework at https://osf.io/byx8r/ and http://guoyang.work/EMEEGStudy.html. The data structure and usage can be found within these links. For any additional information or specific requests, please contact the corresponding author at jhhsiao@ust.hk.

Code availability

The custom codes for EEG decoding and eye movement analysis of this study are publicly available on the Open Science Framework at https://osf.io/byx8r/ and http://guoyang.work/EMEEGStudy.html. The EMHMM analysis codes are available at http://visal.cs.cityu.edu.hk/research/emhmm/. For further details or specific queries regarding the code, please contact the corresponding author at jhhsiao@ust.hk.

Received: 19 June 2024; Accepted: 8 April 2025;
Published online: 12 May 2025

References

1. Arizpe, J., Walsh, V., Yovel, G. & Baker, C. I. The categories, frequencies, and stability of idiosyncratic eye-movement patterns to faces. *Vis. Res.* **141**, 191–203 (2017).
2. Abudarham, N., Shkiller, L. & Yovel, G. Critical features for face recognition. *Cognition* **182**, 73–83 (2019).
3. Royer, J. et al. Greater reliance on the eye region predicts better face recognition ability. *Cognition* **181**, 12–20 (2018).
4. Hills, P. J., Eaton, E. & Pake, J. M. Correlations between psychometric schizotypy, scan path length, fixations on the eyes and face recognition. *Q J. Exp. Psychol.* **69**, 611–625 (2016).
5. Hsiao, J. H. W. & Cottrell, G. Two fixations suffice in face recognition. *Psychol. Sci.* **19**, 998–1006 (2008).
6. Peterson, M. F. & Eckstein, M. P. Individual differences in eye movements during face identification reflect observer-specific optimal points of fixation. *Psychol. Sci.* **24**, 1216–1225 (2013).
7. Davis, J. et al. Social and attention-to-detail subclusters of autistic traits differentially predict looking at eyes and face identity recognition ability. *Br. J. Psychol.* **108**, 191–219 (2017).
8. Quinn, B. P. A. & Wiese, H. The role of the eye region for familiar face recognition: Evidence from spatial low-pass filtering and contrast negation. *Q. J. Exp. Psychol.* **76**, 338–349 (2023).
9. Wilmer, J. B. Individual differences in face recognition: a decade of discovery. *Curr. Dir. Psychol. Sci.* **26**, 225–230 (2017).
10. Chuk, T., Chan, A. B., Shimojo, S. & Hsiao, J. H. Eye movement analysis with switching hidden Markov models. *Behav. Res. Methods* **52**, 1026–1043 (2020).
11. Kanan, C., Bseiso, D. N. F., Ray, N. A., Hsiao, J. H. & Cottrell, G. W. Humans have idiosyncratic and task-specific scanpaths for judging faces. *Vis. Res.* **108**, 67–76 (2015).
12. Peterson, M. F. & Eckstein, M. P. Looking just below the eyes is optimal across face recognition tasks. *Proc. Natl. Acad. Sci. USA* **109**, E3314–E3323 (2012).
13. Mehoudar, E., Arizpe, J., Baker, C. I. & Yovel, G. Faces in the eye of the beholder: Unique and stable eye scanning patterns of individual observers. *J. Vis.* **14**, 6 (2014).
14. Chuk, T., Chan, A. B. & Hsiao, J. H. Understanding eye movements in face recognition using hidden Markov models. *J. Vis.* **14**, 8 (2014).
15. Hsiao, J. H., Lan, H., Zheng, Y. Y. & Chan, A. B. Eye movement analysis with hidden Markov models (EMHMM) with co-clustering. *Behav. Res. Methods* **53**, 2473–2486 (2021).
16. Chuk, T., Chan, A. B. & Hsiao, J. H. Is having similar eye movement patterns during face learning and recognition beneficial for recognition performance? Evidence from hidden Markov modeling. *Vis. Res.* **141**, 204–216 (2017).
17. Chuk, T., Crookes, K., Hayward, W. G., Chan, A. B. & Hsiao, J. H. Hidden Markov model analysis reveals the advantage of analytic eye movement patterns in face recognition across cultures. *Cognition* **169**, 102–117 (2017).
18. Zhang, J. X., Chan, A. B., Lau, E. Y. Y. & Hsiao, J. H. Individuals with insomnia misrecognize angry faces as fearful faces while missing the eyes: an eye-tracking study. *Sleep* **42**, zsy220 (2019).
19. An, J. & Hsiao, J. H. Modulation of mood on eye movement and face recognition performance. *Emotion* **21**, 617–630 (2021).
20. Hsiao, J. H., An, J., Zheng, Y. & Chan, A. B. Do portrait artists have enhanced face processing abilities? Evidence from hidden Markov modeling of eye movements. *Cognition* **211**, 104616 (2021).

21. Hsiao, J. H., An, J., Hui, V. K. S., Zheng, Y. & Chan, A. B. Understanding the role of eye movement consistency in face recognition and autism through integrating deep neural networks and hidden Markov models. *npj Sci. Learn.* **7**, 28 (2022).
22. Hsiao, J. H., An, J. & Chan, A. B. The Role of Eye Movement Consistency in Learning to Recognise Faces: Computational and Experimental Examinations. In (Eds Denison, S., Mack, M., Xu, Y., & Armstrong, B. C.) *Proceedings of the 42nd Annual Conference of the Cognitive Science Society* pp. 1072–1078 (Cognitive Science Society, 2020).
23. da Silva, F. L. EEG and MEG: relevance to neuroscience. *Neuron* **80**, 1112–1128 (2013).
24. Li, A. et al. Neural fragility as an EEG marker of the seizure onset zone. *Nat. Neurosci.* **24**, 1465–1474 (2021).
25. Huang, W. Y. et al. Revisiting the earliest electrophysiological correlate of familiar face recognition. *Int. J. Psychophysiol.* **120**, 42–53 (2017).
26. Ratner, K. G. & Amodio, D. M. Seeing "us vs. them": minimal group effects on the neural encoding of faces. *J. Exp. Soc. Psychol.* **49**, 298–301 (2013).
27. Eimer, M., Gosling, A. & Duchaine, B. Electrophysiological markers of covert face recognition in developmental prosopagnosia. *Brain* **135**, 542–554 (2012).
28. Coronel, J. C. & Federmeier, K. D. The N400 reveals how personal semantics is processed: insights into the nature and organization of self-knowledge. *Neuropsychologia* **84**, 36–43 (2016).
29. Goesaert, E. & Op de Beeck, H. P. Representations of facial identity information in the ventral visual stream investigated with multivoxel pattern analyses. *J. Neurosci.* **33**, 8549–8558 (2013).
30. Kriegeskorte, N., Formisano, E., Sorger, B. & Goebel, R. Individual faces elicit distinct response patterns in human anterior temporal cortex. *Proc. Natl. Acad. Sci. USA* **104**, 20600–20605 (2007).
31. Nemrodov, D., Niemeier, M., Mok, J. N. Y. & Nestor, A. The time course of individual face recognition: a pattern analysis of ERP signals. *Neuroimage* **132**, 469–476 (2016).
32. Cauchoix, M., Barragan-Jason, G., Serre, T. & Barbeau, E. J. The neural dynamics of face detection in the wild revealed by MVPA. *J. Neurosci.* **34**, 846–854 (2014).
33. Mares, I. et al. Face recognition ability is manifest in early dynamic decoding of face-orientation selectivitydEvidence from multi-variate pattern analysis of the neural response. *Cortex* **159**, 299–312 (2023).
34. Noah, S. et al. Neural mechanisms of attentional control for objects: decoding eeg alpha when anticipating faces, scenes, and tools. *J. Neurosci.* **40**, 4913–4924 (2020).
35. Balconi, M. & Lucchiari, C. in *Proceedings of the Annual Meeting of the Cognitive Science Society* (University of California, 2024).
36. Zheng, W. L., Zhu, J. Y. & Lu, B. L. Identifying stable patterns over time for emotion recognition from EEG. *IEEE T. Affect Comput.* **10**, 417–429 (2019).
37. Zion-Golumbic, E., Kutas, M. & Bentin, S. NeuraL DYNAMICS ASSOCIATED WITH SEMANTIC AND EPISODIC MEMORY FOR FACES: EVIDENCE FROM MULTIPLE FREQUENCY BANds. *J. Cogn. Neurosci.* **22**, 263–277 (2010).
38. Fink, A., Grabner, R. H., Neuper, C. & Neubauer, A. C. EEG alpha band dissociation with increasing task demands. *Cogn. Brain Res* **24**, 252–259 (2005).
39. Klimesch, W., Doppelmayr, M. & Hanslmayr, S. Upper alpha ERD and absolute power: their meaning for memory performance. *Prog. Brain Res.* **159**, 151–165 (2006).
40. Ghosh, L., Dewan, D., Chowdhury, A. & Konar, A. Exploration of face-perceptual ability by EEG induced deep learning algorithm. *Biomed. Signal Proces.* **66**, 102368 (2021).
41. Liu, G. Y. et al. EEG-based familiar and unfamiliar face classification using filter-bank differential entropy features. *IEEE T. Hum-Mach. Syst*. https://doi.org/10.1109/Thms.2023.3332209 (2023).
42. Liu, G. Y., Zhang, D., Tian, L. & Zhou, W. D. EEG-based familiar and unfamiliar face classification using differential entropy feature. In *Proc. of the 2021 IEEE International Conference on Human-Machine Systems (Ichms)*, 190–192 (iEEE, 2021); https://doi.org/10.1109/Ichms53169.2021.9582641.
43. William, F. & Aygun, R. ConvoForest classification of new and familiar faces using EEG, 274–279 (IEEE ICSC, 2022); https://doi.org/10.1109/Icsc52841.2022.00052.
44. Nemrodov, D., Anderson, T., Preston, F. F. & Itier, R. J. Early sensitivity for eyes within faces: a new neuronal account of holistic and featural processing. *Neuroimage* **97**, 81–94 (2014).
45. Parkington, K. B. & Itier, R. J. One versus two eyes makes a difference! Early face perception is modulated by featural fixation and feature context. *Cortex* **109**, 35–49 (2018).
46. Bentin, S., Allison, T., Puce, A., Perez, E. & McCarthy, G. Electrophysiological studies of face perception in humans. *J. Cogn. Neurosci.* **8**, 551–565 (1996).
47. Itier, R. J., Latinus, M. & Taylor, M. J. Face, eye and object early processing: What is the face specificity?. *Neuroimage* **29**, 667–676 (2006).
48. Taylor, M. J., Edmonds, G. E., McCarthy, G. & Allison, T. Eyes first! Eye processing develops before face processing in children. *Neuroreport* **12**, 1671–1676 (2001).
49. Naples, A. J., Wu, J., Mayes, L. C. & McPartland, J. C. Event-related potentials index neural response to eye contact. *Biol. Psychol.* **127**, 18–24 (2017).
50. Latinus, M. & Taylor, M. J. Face processing stages: impact of difficulty and the separation of effects. *Brain Res.* **1123**, 179–187 (2006).
51. Smith, F. W. & Smith, M. L. Decoding the dynamic representation of facial expressions of emotion in explicit and incidental tasks. *Neuroimage* **195**, 261–271 (2019).
52. Li, C. L., Burton, A. M., Ambrus, G. G. & Kovács, G. A neural measure of the degree of face familiarity. *Cortex* **155**, 1–12 (2022).
53. Magosso, E., De Crescenzio, F., Ricci, G., Piastra, S. & Ursino, M. EEG alpha power is modulated by attentional changes during cognitive tasks and virtual reality immersion. *Comput. Intel. Neurosci.* **2019**, 7051079 (2019).
54. Sauseng, P. et al. A shift of visual spatial attention is selectively associated with human EEG alpha activity. *Eur. J. Neurosci.* **22**, 2917–2926 (2005).
55. Chan, C. Y. H., Chan, A. B., Lee, T. M. C. & Hsiao, J. H. Eye-movement patterns in face recognition are associated with cognitive decline in older adults. *Psychon. B Rev.* **25**, 2200–2207 (2018).
56. Friedman, D. & Johnson, R. Event-related potential (ERP) studies of memory encoding and retrieval: a selective review. *Microsc. Res. Tech.* **51**, 6–28 (2000).
57. Guillaume, F. & Thomas, É Recollection and familiarity in schizophrenia: an ERP investigation using face recognition exclusion tasks. *Psychiatry Res.* **302**, 113973 (2021).
58. Mograss, M. A., Guillem, F. & Stickgold, R. Individual differences in face recognition memory: comparison among habitual short, average, and long sleepers. *Behav. Brain Res.* **208**, 576–583 (2010).
59. Sun, D. L., Chan, C. C. H. & Lee, T. M. C. Identification and classification of facial familiarity in directed lying: an ERP study. *PLoS One* **7**, e31250 (2012).
60. Bae, G. Y. & Luck, S. J. Dissociable decoding of spatial attention and working memory from EEG oscillations and sustained potentials. *J. Neurosci.* **38**, 409–422 (2018).
61. Bae, G. Y. & Luck, S. J. Decoding motion direction using the topography of sustained ERPs and alpha oscillations. *Neuroimage* **184**, 242–255 (2019).
62. Bilker, W. B. et al. Development of abbreviated nine-item forms of the Raven's standard progressive matrices test. *Assessment* **19**, 354–369 (2012).

63. Zakharov, I., Tabueva, A., Adamovich, T., Kovas, Y. & Malykh, S. Alpha band resting-state EEG connectivity is associated with non-verbal intelligence. *Front. Hum. Neurosci.* **14**, 10 (2020).
64. Woolnough, O. et al. Category selectivity for face and scene recognition in human medial parietal cortex. *Curr. Biol.* **30**, 2707–270 (2020).
65. Yan, X. Q., Liu-Shuang, J. & Rossion, B. Effect of face-related task on rapid individual face discrimination. *Neuropsychologia* **129**, 236–245 (2019).
66. Benedek, M., Schickel, R. J., Jauk, E., Fink, A. & Neubauer, A. C. Alpha power increases in right parietal cortex reflects focused internal attention. *Neuropsychologia* **56**, 393–400 (2014).
67. Rossion, B. et al. A network of occipito-temporal face-sensitive areas besides the right middle fusiform gyrus is necessary for normal face processing. *Brain* **126**, 2381–2395 (2003).
68. Pitcher, D., Walsh, V. & Duchaine, B. The role of the occipital face area in the cortical face perception network. *Exp. Brain Res.* **209**, 481–493 (2011).
69. Alzueta, E., Melcón, M., Jensen, O. & Capilla, A. The 'Narcissus Effect': top–down alpha–beta band modulation of face-related brain areas during self-face processing. *Neuroimage* **213**, 116754 (2020).
70. Deiber, M. P., Ibañez, V., Missonnier, P., Rodriguez, C. & Giannakopoulos, P. Age-associated modulations of cerebral oscillatory patterns related to attention control. *Neuroimage* **82**, 531–546 (2013).
71. Morillas-Romero, A., Tortella-Feliu, M., Bornas, X. & Aguayo-Siquier, B. Resting parietal electroencephalogram asymmetries and self-reported attentional control. *Clin. Eeg Neurosci.* **44**, 188–192 (2013).
72. Palva, S. & Palva, J. M. New vistas for α-frequency band oscillations. *Trends Neurosci.* **30**, 150–158 (2007).
73. Bentin, S. & Deouell, L. Y. Structural encoding and identification in face processing: ERP evidence for separate mechanisms. *Cogn. Neuropsychol.* **17**, 35–54 (2000).
74. Caharel, S., Fiori, N., Bernard, C., Lalonde, R. & Rebaï, M. The effects of inversion and eye displacements of familiar and unknown faces on early and late-stage ERPs. *Int J. Psychophysiol.* **62**, 141–151 (2006).
75. Caharel, S., Ramon, M. & Rossion, B. Face familiarity decisions take 200 msec in the human brain: electrophysiological evidence from a Go/No-go speeded task. *J. Cogn. Neurosci.* **26**, 81–95 (2014).
76. Keyes, H., Brady, N., Reilly, R. B. & Foxe, J. J. My face or yours? Event-related potential correlates of self-face processing. *Brain Cogn.* **72**, 244–254 (2010).
77. Hsiao, J. H. & Chan, A. B. Visual attention to own- versus other-race faces: Perspectives from learning mechanisms and task demands. *British J. Psychol.* **114**, 17–20 (2023).
78. Dimigen, O. Optimizing the ICA-based removal of ocular EEG artifacts from free viewing experiments (retracted article). *Neuroimage* **207**, 116117 (2020).
79. Plöchl, M., Ossandón, J. P. & König, P. Combining EEG and eye tracking: identification, characterization, and correction of eye movement artifacts in electroencephalographic data. *Front. Hum. Neurosci.* **6**, 278 (2012).
80. Dimigen, O., Valsecchi, M., Sommer, W. & Kliegl, R. Human microsaccade-related visual brain responses. *J. Neurosci.* **29**, 12321–12331 (2009).
81. Duncan, D. H., van Moorselaar, D. & Theeuwes, J. Pinging the brain to reveal the hidden attentional priority map using encephalography. *Nat. Commun.* **14**, 4749 (2023).
82. Dimigen, O., Sommer, W., Hohlfeld, A., Jacobs, A. M. & Kliegl, R. Coregistration of eye movements and EEG in natural reading: analyses and review. *J. Exp. Psychol. Gen.* **140**, 552–572 (2011).
83. McKone, E. Holistic processing for faces operates over a wide range of sizes but is strongest at identification rather than conversational distances. *Vis. Res.* **49**, 268–283 (2009).
84. Lau, E. Y. Y., Eskes, G. A., Morrison, D. L., Rajda, M. & Spurr, K. F. Executive function in patients with obstructive sleep apnea treated with continuous positive airway pressure. *J. Int. Neuropsychol. Soc.* **16**, 1077–1088 (2010).
85. Phillips, L. H., Wynn, V. E., McPherson, S. & Gilhooly, K. J. Mental planning and the Tower of London task. *Q. J. Exp. Psychol. A* **54**, 579–597 (2001).
86. Raven, J. The Raven's progressive matrices: change and stability over culture and time. *Cogn. Psychol.* **41**, 1–48 (2000).
87. Chan, S. K. W. et al. Explicit and implicit mentalization of patients with first-episode schizophrenia: a study of self-referential gaze perception with eye movement analysis using hidden Markov models. *Eur. Arch. Psychiatry Clin. N.* **272**, 1335–1345 (2022).
88. Zheng, Y. & Hsiao, J. H. Differential audiovisual information processing in emotion recognition: an eye-tracking study. *Emotion* **23**, 1028 (2023).
89. Coviello, E., Chan, A. B. & Lanckriet, G. R. G. Clustering hidden Markov models with variational HEM. *J. Mach. Learn Res.* **15**, 697–747 (2014).
90. Hsiao, J. H., Chan, A. B., An, J., Yeh, S.-L. & Jingling, L. Understanding the collinear masking effect in visual search through eye tracking. *Psycho. Bull. Rev.* **28**, 1933–1943 (2021).
91. Hsiao, J. H. W., Liao, W. Y. & Tso, R. V. Impact of mask use on face recognition: an eye-tracking study. *Cogn. Res.* **7**, 32 (2022).
92. Liao, W. & Hsiao, J. H. Does word boundary information facilitate Chinese sentence reading in children as beginning readers? *Learning and Instruction* **95**, 102034 (2025).
93. Liao, W. & Hsiao, J. H. Understanding the role of eye movement pattern and consistency in isolated english word reading through hidden Markov modeling. *Cogn. Sci.* **48**, e13489 (2024).
94. Qi, R., Zheng, Y., Yang, Y., Cao, C. C., & Hsiao, J. H. (2024) Explanation strategies in humans versus current explainable artificial intelligence: Insights from image classification. *British J. Psychol.* https://doi.org/10.1111/bjop.12714
95. Cover, T. M. & Thomas, J. A. Entropy, relative entropy and mutual information. *Elem. Inf. Theory* **2**, 12–13 (1991).
96. Branston, N. M., El-Deredy, W. & McGlone, F. P. Changes in neural complexity of the EEG during a visual oddball task. *Clin. Neurophysiol.* **116**, 151–159 (2005).
97. Pinegger, A., Wriessnegger, S. C., Faller, J. & Müller-Putz, G. R. Evaluation of different EEG acquisition systems concerning their suitability for building a brain-computer interface: case. *Stud. Front. Neurosci. Switz.* **10**, 441 (2016).
98. Pion-Tonachini, L., Makeig, S. & Kreutz-Delgado, K. Crowd labeling latent Dirichlet allocation. *Knowl. Inf. Syst.* **53**, 749–765 (2017).
99. Feldman, M. Hilbert transform in vibration analysis. *Mech. Syst. Signal Pr.* **25**, 735–802 (2011).
100. Manjula, M., Mishra, S. & Sarma, A. V. R. S. Empirical mode decomposition with Hilbert transform for classification of voltage sag causes using probabilistic neural network. *Int. J. Elec Power* **44**, 597–603 (2013).
101. Wang, P. Y., Yang, Z. H., Lei, Y. W., Ying, Y. M. & Zhang, H. Differentially private empirical risk minimization for AUC maximization. *Neurocomputing* **461**, 419–437 (2021).
102. Marsaglia, G., Tsang, W. W. & Wang, J. Evaluating Kolmogorov's distribution. *J. Stat. Softw.* **8**, 1–4 (2003).
103. Groppe, D. *fdr_bh* https://www.mathworks.com/matlabcentral/fileexchange/27418-fdr_bh (2020).
104. Benjamini, Y. & Yekutieli, D. False discovery rate-adjusted multiple confidence intervals for selected parameters. *J. Am. Stat. Assoc.* **100**, 71–81 (2005).
105. Benjamini, Y. & Hochberg, Y. Controlling the false discovery rate: a practical and powerful approach to multiple testing. *J. R. Stat. Soc. Ser. B* **57**, 289–300 (1995).

106. Chang, Y.-W. & Lin, C.-J. in *Causation and prediction challenge* 53–64 (PMLR, 2008).
107. Wadkar, M., Di Troia, F. & Stamp, M. Detecting malware evolution using support vector machines. *Expert Syst. Appl.* **143**, 113022 (2020).

Acknowledgements
We are grateful to the Research Grant Council of Hong Kong (GRF #17608621 and CRF #C7129-20G to Janet H. Hsiao), the National Natural Science Foundation of China (no. 62401342 to Guoyang Liu), and the Natural Science Foundation of Shandong Province (no. ZR2024QF092 to Guoyang Liu). We thank Yunke Chen and Yumeng Yang for their help in data preprocessing and data collection.

Author contributions
G.L.: Writing—original draft, methodology, software, investigation, validation, and formal analysis. Y.Y.Z.: Writing—original draft, methodology, data curation, formal analysis, investigation, and validation. M.T.: Writing—original draft, methodology, data curation, and formal analysis. Y.Zh: formal analysis. J.H.H.: conceptualization, writing—review and editing, supervision, project administration, funding acquisition, resources, data curation, and methodology. All authors read and approved the submitted version.

Competing interests
The authors declare no competing financial and/or non-financial interests.

Additional information
Supplementary information The online version contains supplementary material available at https://doi.org/10.1038/s41539-025-00316-3.

Correspondence and requests for materials should be addressed to Janet H. Hsiao.